Towards low audible noise drives for FEV applications

D. Franck, M. van der Giet and K. Hameyer

Institute of Electrical Machines, RWTH Aachen University, D-52062 Aachen, Germany,
e-mail: *david.franck@iem.rwth-aachen.de*

***Abstract*– This paper presents the required steps for the multiphysics acoustic simulation of electrical machines to evaluate its noise behaviour. The proposed scheme is of particular interest for the design and development of electrical drives for full electric vehicles (FEV), because it allows predicting the acoustic characteristic before building a prototype. This numerical approach starts with the electromagnetic force-wave simulation. The computation by a structure dynamic model determines the deformation of the mechanical structure due to the force-waves. The final step of the simulation approach consists of the computation of the excited acoustic radiation. Here, particular attention is paid to the structural-dynamic model. Modelling of microstructures, such as the laminated iron core or insulated coils, is memory and computational expensive. A systematic material homogenisation technique, based on experimental- and numerical modal analyses, yields a higher accuracy at lower computational costs when compared to standard numerical approaches. The presented multiphysics simulation is validated by measurements. The proposed methods are presented by means of a realistic and technically relevant case study.**

***Keywords*— electrical machines, electromagnetic simulation, structure-dynamic simulation, multi-physics, noise and vibration evaluation.**

I. INTRODUCTION

The continuous discussion about ecological aspects and the awareness of the shortage of fossil fuel promote the research for alternative drives for cars. In the recent years hybrid electric cars are accepted to combine higher energy efficiency with constant or even improved driving comfort. In order to reduce the CO2 emission in urban environments full electric vehicles present a valid option. The recent improvements in battery technologies promote the development of such cars, as can be seen in the increasing number of electric prototypes and even small batch production of electric vehicles.

However, cars are highly emotional products, where not only the efficiency, performance and design, but also the acoustic characteristics contribute to the customers' purchase decision. The familiar sound of a car changes with the electrification of the engine from broadband noise to annoying single tones. Even with a strongly reduced emitted sound power level, these single tones can be sensed to be extraordinary annoying. Therefore, the acoustic radiation of the electric drive trains for vehicles is to be reduced to a minimum.

In order to predict the acoustic characteristic before building a prototype, accurate and automated numerical simulations are required. In this paper a multi-physics simulation approach, applying weak numerical coupling of the underlying models, is applied. As an example a case study with an permanent magnet synchronous motor is presented in this paper. In this regards, a coupling of electromagnetic simulation to determine the magnetically exciting forces, which act on the stator of the machine and a structural-dynamic simulation to calculate the displacement of the stator surface is established. A flow chart of the mentioned simulation chain is presented in Fig. 1.

In contrast to classical approaches [5] the mechanical material parameters of laminated stator iron core is homogenised for the structural-dynamic model. By experimental and numeric modal analysis the mechanical material parameters, Youngs' modulus, Poisson ratio and shear modulus, are determined by applying an optimisation algorithm. This results in a significant improvement in the model accuracy and reduces the computational costs of the structural-dynamic simulation. The aim of the multi-physical model presented here, is the prediction of the acoustic behaviour of the studied servo drive.

II. ELECTROMAGNETIC SIMULATION

The essential part of the multi-physics simulation approach is the electromagnetic computation since the electromagnetic field generates force-waves exciting the stator lamination and housing of the drive motor.

Classical analytical approaches [7], [8] allow for the determination of spatial- and temporal orders of the excited flux density waves. A linear time invariant behaviour of the machine is assumed and all field components are approximated with rectangular functions. Different field components, such as the spatial or parametric harmonics, slotting and winding space harmonics, harmonics caused by the teeth saturation, eccentricity fields, etc., can be modelled separately. The spatial- and temporal orders of the excited force density waves are determined by combination of two of the previous mentioned field components. The properties of the force density waves and their source flux density waves can be presented in so called excitation tables [8]. As an example an extract of the excitation table for the interaction of the fields generated by stator winding space harmonics and rotor space harmonics is presented in table I, whereby

$$\nu_1 = p\left(\frac{2mg}{N_q} - 1\right), g = 0,\pm1,\pm2,\ldots \quad (1)$$

and

$$\nu_2 = p(2k+1), k = 0,\pm1,\pm2,\ldots \quad (2)$$

describe the spatial order of the flux density wave of the stator winding space harmonics and rotor space harmonics respectively. The ordinal numbers are presented in the first row and first column. The spatial and temporal order of the generated force density wave is given in the table body. With this kind of tables a first assumption about the excited force waves is done. These results are important for the further studies. On the one hand the numeric model can be validated, on the other hand a determination of the noise sources is possible as also done in [12].

Due to the homogenous structure in axial direction of the studied motor, a two dimensional magnetic finite element (FE) model is applied. The flux density distribution is calculated for one rotation of the rotor with a mechanical

TABLE I.
EXCITATION TABLE: STATOR WINDING SPACE HARMONICS AND ROTOR SPACE HARMONICS.

ν_1	-7	29	-13	35	temporal order of σ
ν_2					
11	4		-2		22
-11					0
33					44
-33		-4		2	-22
55					66
-55					-44

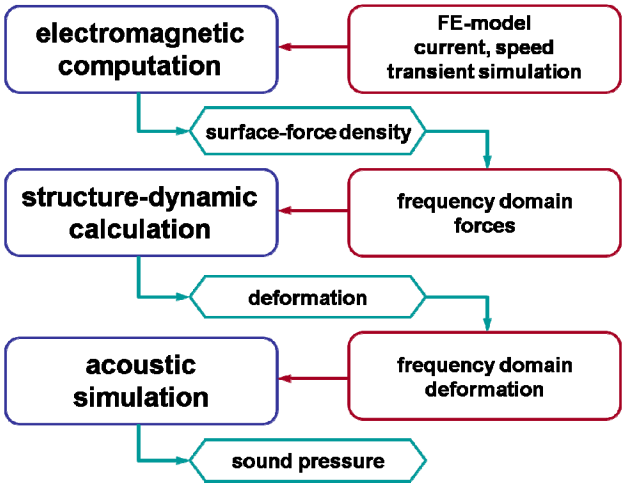

Fig. 1. Flow chart representing the multiphysics simulation approach.

rotation angle of one degree per step. The next computational steps are distinguished into analyses of noise sources and the computation of the electromagnetically excited force-waves acting at the stator of the machine. To study the sources of the electromagnetically excited noise in a first step, only the normal component of the flux density waves is considered. This simplification is valid, because the magnitude of the normal components is dominant when compared to the tangential component. The aim of this analysis step is not to exactly determine force-wave magnitudes and associated phase angles, but to identify the cause of particular electromagnetic force excitations.

The resulting air gap field is studied in frequency and pole domain. Therefore, the air gap flux density is modal decomposed by a 2D-DFT in space and time. It hence, can be described by a Fourier-series with the magnitude $B_{i,j}$ of each flux density wave, the ordinal number ν_j, the frequency f_i and the phase angle $\varphi_{i,j}$ by:

$$B(x,t) = \sum_{i=-i_{\max}}^{i_{\max}} \sum_{j=1}^{j_{\max}} B_{i,j} \cdot \cos\left(2\pi f_i \cdot t - \nu_j \cdot x - \varphi_{i,j}\right) \quad (3)$$

Whereby i represents the frequency order, i_{max} is determined by the number of calculated simulation steps per period, j represents the circumferential order and j_{max} is given by the number of flux density samples in the air gap.

In contrast to the classical approaches [7], [8], in which the force density is Fourier-decomposed after calculating it by the multiplication of the flux density in the time domain, here the force density waves σ are determined by

applying a convolution of the flux density waves with themselves [6].
In this case, the simplified Maxwell stress tensor is applied, not considering the tangential flux density components. A representation of the numerically sampled force density waves as a Fourier-series can be given by:

$$\sigma(x,t) = \sum_{k=1}^{k_{\max}} \sum_{l=1}^{l_{\max}} \hat{\sigma}_{k,l} \cdot \cos\left(2\pi\left(f_k \pm f_l\right)\cdot t - \left(\nu_k \pm \nu_l\right)\cdot x - \left(\varphi_k \pm \varphi_l\right)\right). \quad (4)$$

With this approach, a decomposition of the force-density waves into trigonometric combinations of flux density waves is possible.
Combining both, the numeric and analytic approaches, gives a in-depth insight into the generation and cause of the force density waves [6], [13]. With this knowledge a manipulation and therefore minimisation or eventually cancellation of the noise excitation is possible. This Fourier-decomposed force density waves are studied individually for each frequency and ordinal number. In the following, the resultant force density wave with the frequency equal to two times the pole-pair number p und the circumferential mode $\nu = 2$ are presented as an example. This particular force density wave σ_{tot} and its decomposition in the three most important components σ_A, σ_B and σ_C is depicted in a space vector diagram (Fig. 2). It has to be noted that all less significant, respectively small components, which are not drawn in Fig. 2, will close the gap between the tip of the vectors σ_{tot} and σ_C.

The dominant force density wave component σ_A can be identified as superposition of the combination of the flux density waves of stator winding- and rotor space harmonics, as well as the stator space harmonics and the reluctance field due to the slotting effects. The frequencies and ordinal numbers of the flux density waves, which are involved in the generation of σ_A, σ_B and σ_C are collected in table II. The decomposition of these three force waves into flux-density waves is collected in table III. The flux density waves are mapped to the before mentioned sources and are defined by frequency and pole-pair number. The result of this analysis step is the determination of the most significant noise sources and their interpretation respective cause. These results are used for the acoustic optimisation of the studied motor. In particular, the winding scheme, rotor pole-pair number and the stator's slot number are sensitive parameters concerning the noise excitation of this motor.

In the next step, the surface-force density is calculated from the flux density distribution by using the Maxwell-stress tensor applied in the time domain. In contrast to the previous analysis step of the electromagnetic noise causes, both, the normal and tangential components of the flux density are considered. For the multiphysics simulation chain the influence of the tangential flux density component is significant, particularly the phase angle of the force density waves is important. The flux density is evaluated on the interface between the air gap and the iron stator teeth. In this way the non-linear characteristics of the iron can be taken into account.

III. MATERIAL PARAMETER OPTIMISATION

The deformation of the stator can be calculated from the calculated force densities acting on the stator teeth. The vibrational behaviour of the stator system is strongly dependent on its material properties [3]. Therefore a detailed knowledge of all associated material parameters is required. In general, mechanical material parameters for structures, such as laminated iron cores or insulated coils, are unknown. Hence, the material parameters have to be identified by measurements or have to be estimated [10], [11]. Here, a material homogenisation technique is applied to cope with this material parameter issue. The mechanical material parameter Youngs' modulus, Poisson ratio and shear modulus are identified based on numerical and experimental modal analysis [1].
The laminated iron core as well as the resined coils is a transverse isotropic structure. These materials are characterised by symmetry in one plane, for example the x-y plane. Hooke's matrix for transverse isotropic materials with the given plane of symmetry is described by:

$$H = \begin{pmatrix} \frac{1}{E_x} & -\frac{\nu_{xy}}{E_x} & -\frac{\nu_{xz}}{E_x} & 0 & 0 & 0 \\ -\frac{\nu_{xy}}{E_x} & \frac{1}{E_x} & -\frac{\nu_{xz}}{E_x} & 0 & 0 & 0 \\ -\frac{\nu_{xz}}{E_x} & -\frac{\nu_{xz}}{E_x} & \frac{1}{E_z} & 0 & 0 & 0 \\ 0 & 0 & 0 & \frac{2\left(1+\nu_{xy}\right)}{E_x} & 0 & 0 \\ 0 & 0 & 0 & 0 & \frac{1}{G_{yz}} & 0 \\ 0 & 0 & 0 & 0 & 0 & \frac{1}{G_{yz}} \end{pmatrix}. \quad (5)$$

In this case, the mechanical material properties can be described by five independent parameters, namely the Youngs' E_x and E_z in x and z direction, the shear modulus G_{yz} in the y-z plane and the Poisson ration ν_{xy} and ν_{xz} in the x-y and the x-z plane.
The homogenised parameters are determined by solving an inverse numerical modal analysis, i.e. optimising these

TABLE II.
ORDINAL NUMBERS AND FREQUENCIES OF IMPORTANT FORCE DENSITY WAVES, WHERE M IS THE NUMBER OF PHASES AND NQ DENOTES THE DENOMINATOR REDUCED FRACTION OF THE SLOT NUMBER PER POLE AND PHASE.

Cause	Circumferential ordinal number	Frequency order
1. stator winding space harmonics	$\nu = p\left(\frac{2mg}{N_q} - 1\right), g = 0,\pm1,\pm2,...$	p
2. rotor space harmonics	$\nu = p(2k+1), k = 0,\pm1,\pm2,...$	$(2k+1)$p
3. rotor reluctance field	$\nu = p(2l+1) + N_1, l = 0,\pm1,\pm2,...,$	$(2l+2)$p

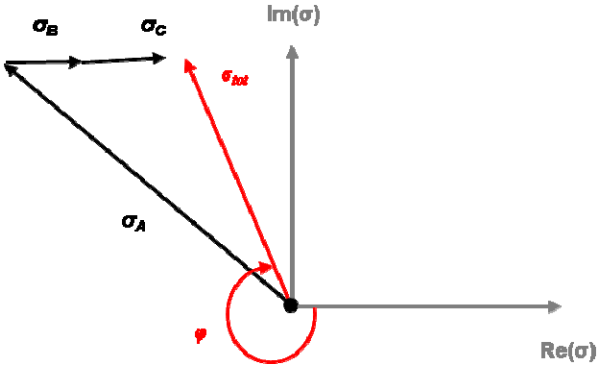

Fig. 2. Space vector representation of the force wave $f=2pf_0$ and $=2$.

TABLE III.
MAPPING OF FORCE DENSITY WAVES TO FLUX DENSITY WAVES.

	f1/f0	ν1	Field	f2/f0	ν2	Field
A	p	-13	3	p	11	1
B	p	35	3	3p	33	2
C	p	-1	1	p	-1	1

parameters in order to fit the resonant frequencies of the numerical modal analysis to the results of the experimental measurements. To solve this inverse problem a Differential Evolution algorithm is applied [9]. The material parameters, their boundary constraints and relative deviation of the first four resonant frequencies of the laminated iron core as well as the material properties of bulk iron as comparison are collected in table IV. The described method can be applied to determine the mechanical material parameters of transversal isotropic materials in general. However, a drawback in this approach is the request of a prototype machine. The resulting material parameters from the discussed approach are used in a next step for the structural-dynamic simulation.

TABLE IV.
OPTIMISED MATERIAL PARAMETERS AND DEVIATION OF THE FIRST 4 RESONANT FREQUENCIES.

Parameter	Laminated core	Bulk iron	Max	Min
Ex	212.7 GPa	210 GPa	250 GPa	100 GPa
Ez	26.3 GPa	210 GPa	100 GPa	1 GPa
νxy	0.40	0.3	0.6	0.2
νxz	0.14	0.3	0.6	0.01
Gxy	90.2 GPa	80 GPa	100 GPa	10 GPa
Resonant frequencies and relative deviation with material parameter optimization frequencies				
721 Hz	1947 Hz		1575 Hz	3553 Hz
1,9 %	12.3%		0,4 %	1,6 %

IV. STRUCTURAL-DYNAMIC SIMULATION

The structural-dynamic simulation is used to determine the deformation of the machine's stator. In the FE model the deformation is represented by the displacements for each node. In the studied case the structural-dynamic simulation is performed by numerical modal analysis, i.e. finding the eigenvalues of the corresponding eigenproblem. Subsequent modal superposition is applied to determine the deformation for each frequency of significant electromagnetic excitation. For this purpose, a three dimensional model of the complete mechanical structure is developed.

The frequencies for the modal superposition are selected by the magnitude of the force density wave and the eigenvalues of the numerical modal analysis. Since the structural-dynamic simulation is based on a three-dimensional model, the two-dimensional force distribution is transformed from the 2-D electromagnetic mesh to the 3-D structural-dynamic mesh [2].

The set-up of the studied motor is drawn in Fig. 3. In the studied case, the cooling-fins are modelled with a high level of detail, in order to model the mass and the mass distribution as accurate as possible and to provide a detailed description of the radiating surface. The stator is fixed to a rigid surface with four screws. Therefore, the nodes around the screws are connected to node with no degree of freedom by a three-dimensional spring, modelling the input impedance of the drive train.

As performed in the previous example, the same frequency $f=2pf_0$ is chosen to demonstrate the applied approach. The simulated mechanical stress is shown in Fig. 4. The vibration mode *2* is dominant for this frequency. This constellation was predicted with the results from the electromagnetic simulation. The cooling fins are oscillating strongly, which shows the importance of the detailed model. This is especially true when regarding the sound pressure simulation, which will be discussed in the next section.

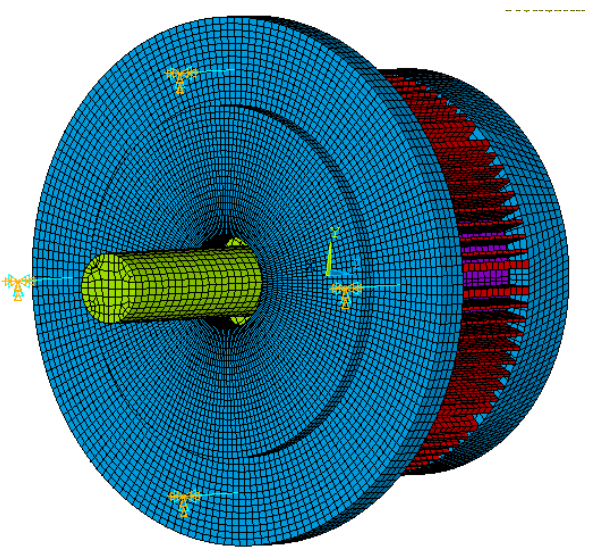

Fig. 3 Structure of the motor and mounting.

V. Results and Validation by Deformation Measurements

The results of the simulation discussed so far is the force distribution acting on the stator's teeth, the deformation of the stator. For the structural-dynamic simulation the fitted material parameters for the homogenised model are used. Deformation measurements are performed to validate the multiphysics simulation chain. The acceleration is measured on the surface of the electrical machine at *16* different positions [4]. Fig. 5 shows the set-up of the practical experiment. The acceleration is measured employing a dual channel signal analyser. One of the two accelerometers is kept at a constant position. The second sensor is placed at various measurement points on the surface of the machine. By double integration of the acceleration $\boldsymbol{a}$, the displacement $\boldsymbol{d}$ at the points can be calculated. The data for the displacement on the surface of the three-dimensional FE model are evaluated at the measured positions. The deformation shape and the magnitudes for the first eight mode numbers are compared.

As an example, the deformation at the studied excitation at frequency $f = 2pf_0$ is presented in Fig. 6. The left diagram illustrates the mode shapes; the right diagram compares the amplitudes of the deformation according to its modal number. The amplitude of dominant deformation with the modal number *2* differs less then *10%* from the measurements and simulation. As expected from the force excitation the mode number of the deformation is $r = 2$. The measurements reveal comparable high amplitude with the mode number one. The reason for this may be found in the eccentricity, for example caused by an eccentric rotor adjustment, or a magnetic anisotropy. Since the frequency

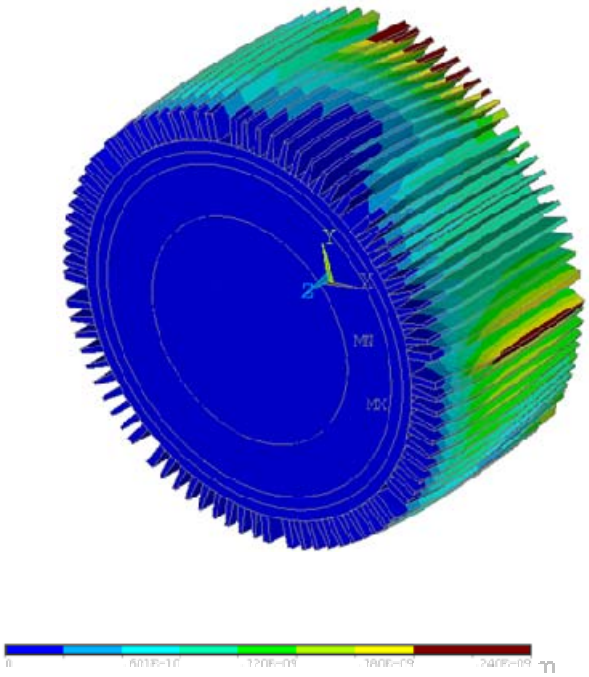

Fig. 4 Deformation of the stator system for the frequency $f=2pf_0$, the front shows the mounting surface.

of the deformation with mode number one is $f = 2pf_0$ the eccentricity is static. Indications for a static eccentricity are also found in other frequency components of the measurements. Static eccentricity is unavoidable in the production of electrical machines.

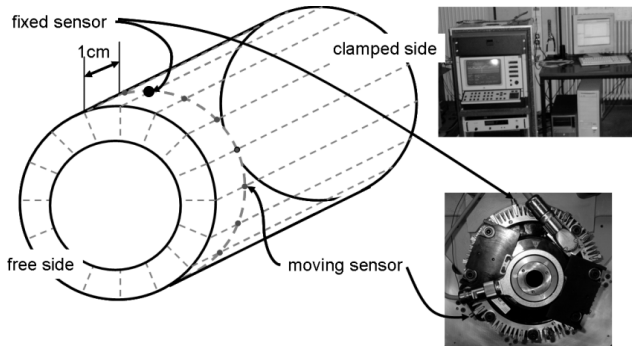

Fig. 5. Experimental set-up for the acceleration measurements.

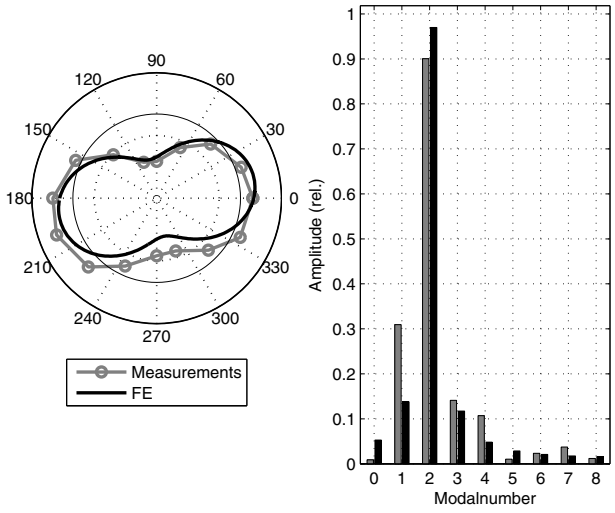

Fig. 6. Comparison of simulation and measurement: Displacement on the surface of the stator with $f=2pf_0$.

VI. CONCLUSIONS

In this paper, the electromagnetic excited structure-borne sound of a permanent magnet synchronous machine is analysed. An automated multi-physics simulation model applying weak numerical coupling is presented and the important aspects for audible noise simulations of electrical machines are pointed out. In particular, the analysis of the electromagnetic forces is discussed. With the combination of analytical and numeric approaches a detailed inside to the force wave generation is given.

With these results an acoustic optimisation of the motor can be performed. This will be the topic of further work from the authors at IEM RWTH Aachen University. In contrast to commonly used mechanical material parameters a material homogenisation is performed for the structural-dynamic simulation. It is shown, that this kind of material parameters yields a very accurate structural dynamic model. The presented approach for the material homogenisation is of general application range. However, it is dependent on the availability of a prototype and required measurement data from it. A generalisation of this approach is planed for future studies.

It can be stated that the results of this simulation with the optimised material parameters are in good agreement with the measurements performed. The simulation model reveals a realistic pattern of the structure-borne sound and acoustic radiation. Therefore, it is possible to benchmark the acoustic behaviour of optimized designs before building a prototype. In the further work the force injection into the drive train of an electric vehicle will be investigated.

VII. REFERENCES

[1] D. Ewins, *Modal Analysis*, Research Studies Press LTD., Baldock, Hertfordshire, England, 2000.

[2] M. Furlan, A. Cernigoj, and M. Boltezar, "A coupled electromagnetic-mechanical-acoustic model of a DC electric motor", *Int. J. Comput. Math. Electr. Electron. Eng*., Vol. 22 No. 4, 2003.

[3] Garvey, S., "The vibrational behaviour of laminated components in electrical machines", *Fourth International Conference on Electrical Machines and Drives*, pp. 226-231, 1989.

[4] G. Genta, *Vibartions of Structures and Machines - Practical Aspects*, Springer-Verlag Berlin Heidelberg, 1999.

[5] J. Gieras, C. Wang, and J. C. Lai , *Noise of Polyphase Electric Motors*, CRC Press Taylor & Francis Group, 2006.

[6] M. van der Giet, R. Rothe, K. Hameyer, "Asymptotic Fourier decomposition of tooth forces in terms of convolved air gap field harmonics for noise diagnosis of electrical machines", *COMPEL*, Vol. 28 No. 4, pp. 804-818, 2009.

[7] M. Herranz Gracia, *Methoden zum Entwurf von robusten Stellantrieben unter Berücksichtigung fertigungsbedingter Abweichungen*, PhD dissertation IEM RWTH Aachen, Shaker Verlag, Aachen, 2008.

[8] H. Jordan, *Geräuscharme Elektromotoren*, W. Girardet, Essen, 1950.

[9] Price, K. and Storn, R., "Differential Evolution: Numerical Optimization Made Easy", *Dr. Dobb's Journal, April 97*, pp. 18 - 24, 1997.

[10] Ramesohl, I.; Henneberger, G.; Kuppers, S. and Hadrys, W., "Three dimensional calculation of magnetic forces and displacements of a claw-pole generator", *IEEE Transactions on Magnetics*, Vol. 32 No. 3, pp. 1685-1688, 1996.

[11] Ramesohl, I, *Numerische Geräuschberechnung von Drehstrom-Klauenpolgeneratoren*, Sahker-Verlag Aachen, 1999.

[12] Shenbo Yu; Renyuan Tang; , "Electromagnetic and mechanical characterizations of noise and vibration in permanent magnet synchronous machines," Magnetics, IEEE Transactions on , vol.42, no.4, pp.1335-1338, April 2006.

[13] M. van der Giet, R. Rothe, M. Herranz Gracia, and K. Hameyer, "Analysis of noise exciting magnetic force waves by means of numerical simulation and a space vector definition," in 18th Internationa Conference on Electrical Machines, ICEM 2008, Vilamoura, Portugal, September 2008.